A Mutant of DNA Polymerase I (Klenow Fragment) with Reduced Fidelity†

Steven S. Carroll, Marlon Cowart, and Stephen J. Benkovic*
Department of Chemistry, The Pennsylvania State University, University Park, Pennsylvania 16802
Received July 11, 1990; Revised Manuscript Received September 19, 1990

ABSTRACT: The kinetic parameters governing incorporation of correct and incorrect bases into synthetic DNA duplexes have been investigated for *Escherichia coli* DNA polymerase I [Klenow fragment (KF)] and for two mutants, Tyr766Ser and Tyr766Phe. Tyr766 is located at the C-terminus of helix O in the DNA-binding cleft of KF. The catalytic efficiency for correct incorporation of dNTP is reduced 5-fold for Tyr766Ser. The catalytic efficiencies of all 12 possible misincorporations have been determined for both KF and Tyr766Ser by using single-turnover kinetic conditions and a form of the enzyme that is devoid of the 3′–5′ exonuclease activity because of other single amino acid replacements. Tyr766Ser displays an increased efficiency of misincorporation (a reduction in fidelity) for several of the 12 mismatches. The largest increase in efficiency of misincorporation for Tyr766Ser occurs for the misincorporation of TMP opposite template guanosine, a 44-fold increase. In contrast, the efficiencies of misincorporation of dAMP opposite template A, G, or C are little affected by the mutation. A determination of the kinetic parameters associated with a complete kinetic scheme has been made for Tyr766Ser. The rate of addition of the next correct nucleotide onto a preexisting mismatch is decreased for Tyr766Ser. The fidelity of Tyr766Phe was not substantially different from that of KF for the misincorporations examined, indicating that it is the loss of the phenolic ring of the side chain of Tyr766 that leads to the significant decrease in fidelity. The results indicate that KF actively participates in the reduction of misincorporations during the polymerization event and that Tyr766 plays an important role in maintaining the high fidelity of replication by KF.

DNA polymerase I (pol I)[1] from *Escherichia coli* is a multifunctional enzyme that carries out synthesis of DNA during replication and repair processes. It contains three distinct activities: DNA polymerase, a 3′–5′ exonuclease, and a 5′–3′ exonuclease, located on separate domains of the enzyme. The large proteolytic fragment [Klenow fragment (KF)] of Pol I retains the polymerase and 3′–5′ exonuclease activities of the native enzyme (Brutlag et al., 1969; Klenow & Henningsen, 1970). These activities act in concert to carry out DNA synthesis with high fidelity.

The kinetic mechanisms describing correct (Kuchta et al., 1987) and incorrect (Kuchta et al., 1988) DNA synthesis by KF have recently been determined, by using as substrates duplexes made from synthetic oligonucleotides of defined sequence. During correct processive synthesis, the rate of incorporation of nucleotides is limited by a conformational change occurring prior to a rapid formation of the chemical bond. During correct nonprocessive synthesis, when the enzyme is forced to dissociate after one round of synthesis, the dissociation rate limits the rate of synthesis. The rate of incorrect synthesis is limited by the rate of the formation of the chemical bond. Three distinct kinetic steps involved in the selection by KF of correct nucleotides were inferred; selection during dNTP binding and phosphodiester bond formation, selection during a step following chemical bond formation that serves to hold mismatched products onto the enzyme for correction by the 3′→5′ exonuclease, and a decreased rate of addition of the next correct base onto the mismatch.

The great majority of the selectivity occurs during the first stage of selection. In order to understand the role of the enzyme in the selection of the correct base and how this selection is communicated to give an increased rate of catalysis for correct over incorrect bases, the study of catalysis by two site-specific mutants of KF, Tyr766Ser and Tyr766Phe, was undertaken. The construction and genetic characterization of the mutants will be discussed elsewhere (Polesky et al., 1990). Tyr766 is located at the C-terminal end of helix O, in the putative DNA-binding cleft of KF (Ollis et al., 1985), and was selected as a site for study on the basis of its labeling by photoaffinity analogues of dNTP (Joyce et al., 1985) and of DNA (Catalano et al., 1990), and by its strict conservation among several polymerases (Lawyer et al., 1989; Leavitt & Ito, 1989; Lopez et al., 1989). Changes in the efficiencies with which Tyr766Ser makes certain mismatches give insight into the importance of this residue in the fidelity of DNA synthesis by KF.

Experimental Procedures

Materials. Pharmacia supplied dNTPs. [α-^{32}P]dNTPs and [γ-^{32}P]ATP were from New England Nuclear. The mutant of KF, Y766S, and the double mutants Y766S, D424A and Y766F, D424A, were purified from overproducing strains supplied by A. Polesky and C. Joyce (Yale University). The purification of Y766S, Y766S(exo–), Y766F(exo–), and KF(exo–) included chromatography on both Biorex 70 and Sephadex G-100 to ensure removal of contaminating exonuclease activities (Joyce & Grindley, 1983). The enzymes were judged to be greater than 95% homogeneous by SDS–PAGE. Assays revealed no exonuclease activity for the exo–

†This work was supported by NIH Postodoctoral Fellowships GM12162 (S.S.C.) and GM12649 (M.C.) and NIH Grant GM13306 (S.J.B.).
* Author to whom correspondence should be addressed.

[1] Abbreviations: pol I, DNA polymerase I from *Escherichia coli*; KF, Klenow fragment of *E. coli* DNA polymerase I; TEAB, triethylammonium bicarbonate; EDTA, (ethylenedinitrilo)tetraacetic acid; SDS–PAGE, sodium dodecyl sulfate–polyacrylamide gel electrophoresis. (exo+) or (exo–) indicates the presence or absence of 3′–5′ exonuclease activity of a particular mutant, respectively, by mutations in the 3′–5′ exonuclease active site as described under Experimental Procedures. If no designation of exonuclease activity is given, the enzyme is exo+. X·Y indicates mismatches with the misincorporated base, X, opposite the template base, Y.

0006-2960/91/0430-804$02.50/0

mutants under reaction conditions employed. Concentrations of enzymes were determined by using $\epsilon_{278} = 6.32 \times 10^4$ M^{-1} cm^{-1} (Setlow et al., 1972). Dr. Jin-Tann Chen provided (S_P)-TTPαS. Cloned T4 polynucleotide kinase was purchased from U.S. Biochemicals.

DNA. DNA oligomers were synthesized on either an Applied Biosystems 380A synthesizer or a Milligen 7500 synthesizer. Oligonucleotides were purified on 20% acrylamide–8 M urea gels, eluted into 1 M TEAB, pH 7.6, and then desalted on Waters Sep-Pak C18 cartridges. DNA duplexes were formed by heating an equimolar mixture of primer and template oligonucleotides to 65 °C for 15 min and then cooling slowly to room temperature over a 2-h period. Quantitation of DNA duplexes was achieved by addition of the next correct [α-^{32}P]dNTP as previously described (Kuchta et al., 1987). DNA duplexes containing a mismatched base at the 3′ end of the primer were quantitated by the same method except the reaction times were extended to 40 min.

Incorporation of radioactive bases into DNA duplexes was followed by the (Whatman) DE-81 filter binding assay as previously described (Bryant et al., 1983).

DNA duplexes and oligomers were 5′-end-labeled with T4 polynucleotide kinase and [γ-^{32}P]ATP as described (Maniatis, 1980). Electrophoretic separation of oligomers was accomplished on denaturing 14 or 20% acrylamide gels containing 8 M urea. Bands corresponding to substrate and product were located by autoradiography, excised from the gel with a razor blade, and counted in 3 mL of Scintiverse II (Fisher) in a Beckman LS6800 or LS8100 scintillation counter.

Kinetic Parameters for Correct Incorporation. The rate of incorporation of the next correct base onto the 13/20mer was determined in a reaction containing a final concentration of 150 nM 13/20mer (5′ end labeled), 10–40 μM dATP, and 400 nM Y766S(exo–) in 50 mM Tris, pH 7.4, and 5 mM $MgCl_2$. Reactions were initiated by combining a solution containing enzyme and substrate DNA with another solution containing Mg·dATP in a rapid quench instrument (Johnson, 1986) and then quenching the reaction with 0.5 M EDTA, pH 7.5, after reaction times ranging from 5 ms to 20 s. All rapid quench experiments were carried out at 21 °C by means of a circulating water bath. A sample of the quenched reaction (10 μL) was combined with an equal volume of gel load buffer, and 10 μL of the resulting solution was electrophoresed on an acrylamide gel. The product band was quantitated as described, and the rate of appearance of product or disappearance of substrate was fit to a single exponential to determine the observed rate. Lineweaver–Burk analysis was used to determine the rate of polymerization, k_{pol}, and K_M (dATP). The off rate for product DNA was determined as previously described (Kuchta et al., 1987). The rate of 3′→5′ exonuclease activity was measured by using 9A/20(A) as substrate. The reaction mixture contained 120 nM 9A/20(A) (5′-end-labeled 9Amer), and 400 nM enzyme was used to initiate the reaction in 50 mM Tris, pH 7.4, and 5 mM $MgCl_2$. After various reaction times an aliquot of the reaction was quenched with gel load buffer and electrophoresed. The bands corresponding to the 9A- and 9mers were quantitated, and the rate of disappearance of 9Amer was fit to a single exponential. All reaction rates determined manually were carried out at ambient temperature (22 °C). The binding constant, K_D, for 13/20(T) and Y766S was determined by reaction of a solution of 20 nM Y766S and from 7 to 100 nM 5′-end-labeled 13/20(T) with a solution of 5mM $MgCl_2$ and 40 μM dATP in 50 mM Tris, pH 7.4, in the rapid quench instrument. The amount of enzyme-bound DNA was quantitated as the amount of DNA turned over during the burst phase of the reaction. The plot of burst amplitude versus 13/20(T) concentration was fit to a quadratic form of the binding equation.

Single-Turnover Misincorporation Reactions. The rate of misincorporation for a given mismatch was determined by mixing 110–150 nM 5′-end-labeled duplex with 20–100 μM dNTP in a solution containing 50 mM Tris, pH 7.4, and 5 mM $MgCl_2$. The reaction was initiated by adding the exo– enzyme to 400 nM. At various times from 15 s to 90 min, a 3-μL aliquot was removed and quenched in 3 μL of gel load buffer. A sample (3 μL) was then loaded on a 20% acrylamide gel. The rate of misincorporation of TTP opposite template G using Y766S(exo–) was too rapid for manual determination and was measured by using the rapid quench instrument.

Steady-State Misincorporation Reactions. Misincorporation of TTP into 10/20(G) [the product of the reaction of 9/20(A) and TTP] was measured by incubating 700 nM 10/20mer, 7.5–30 μM [α-^{32}P]TTP [(0.3–1.0) $\times$ 10^5 cpm/pmol], and 10 nM Y766S(exo–) or 80 nM KF(exo–) or Y766F(exo–) in a reaction containing 50 mM Tris, pH 7.4, and 5 mM $MgCl_2$. Aliquots (3 μL) were withdrawn at various times from 30 s to 20 min and quenched in 3 μL of gel load buffer. Samples (6 μL) were run on acrylamide gels. The bands corresponding to 10Tmer were located by autoradiography, excised, and counted as described above.

Formation of dNMP from dNTP. The rates of production of dNMP from dNTP during misincorporation reactions were determined in reactions containing 100 nM 13/20(G) or 9/20mer, 100 nM enzyme, and 10 μM TTP or dATP (7000 or 16000 cpm/pmol, respectively) in 50 mM Tris, pH 7.4, and 5 mM $MgCl_2$. The reaction was initiated by addition of the enzyme. Aliquots (3 μL) were removed at various times from 1 to 60 min and quenched in 3 μL of 120 mM EDTA, pH 7.5. Samples (2 μL) were spotted on lanes of a poly(ethylenimine) TLC plate (EM Sciences) and developed with 0.3 M KP_i, pH 7. Spots corresponding to TMP or dAMP were located by autoradiography and by comparison to standards, sliced from the TLC, and quantitated by counting in 3 mL of scintillation fluid.

Buildup of 13T/20(G) in the Presence of Exo+ Enzymes. The rate of appearance of mismatched product DNA and the extent to which the mismatched product builds up in the presence of wild-type KF and Y766S mutant which retain the 3′–5′ exonuclease activity were determined in reactions containing 150 nM 5′-end-labeled 13/20(G), 400 nM Y766S or KF, and 2.5–40 μM TTP in 50 mM Tris, pH 7.4, and 5 mM $MgCl_2$. After reaction times ranging from 15 s to 5 min, an aliquot (3 μL) was quenched into an equal volume of gel load buffer, electrophoresed, and quantitated as described.

Extension of Mismatches. Into rate of addition of the next correct nucleotide onto a duplex substrate containing a 3′-terminal mismatch was determined by incubating 110 nM 5′-end-labeled 13T/20(C), 400 nM Y766S(exo–) or KF(exo–), with 10–60 μM TTP in a solution containing 50 mM Tris, pH 7.4, and 5 mM $MgCl_2$. After reaction times from 2 to 100 min for the reaction containing Y766S(exo–) and from 15 to 600 s for the reaction containing KF(exo–), an aliquot of 3 μL was removed and quenched with an equal volume of gel load buffer. A sample was electrophoresed, and the bands corresponding to substrate and product were excised and quantitated as described. Elemental effects on the rate of extension of the 13T/20(C) mismatch were determined by substituting (S_P)-TTPαS (40 or 60 μM) in the same reaction. The rate of extension of 13G/20(T) was measured by using the same conditions, but reaction times varied from 5 ms to

Chart I: DNA Substrates Used[a]

9/20(A)[a]	5'TCGCAGCCG 3'AGCGTCGGCAGGTTCCCAAA5'
13/20(T)	5'TCGCAGCCGTCCA 3'AGCGTCGGCAGGTTCCCAAA5'
13/20(G)	5'TCGCAGCCGTCCT 3'AGCGTCGGCAGGAGCCCAAA5'
13/20(C)	5'TCGCAGCCGTCCT 3'AGCGTCGGCAGGACACCAAA5'
9A/20(A)[b]	5'TCGCAGCCGA 3'AGCGTCGGCAGGTTCCCAAA5'
13T/20(C)	5'TCGCAGCCGTCCTT 3'AGCGTCGGCAGGACACCAAA5'
13G/20(T)	5'TCGCAGCCGTCCAG 3'AGCGTCGGCAGGTTCCCAAA5'

[a] The name of each duplex is given as the lengths of primer/template, followed by the next available template base in parentheses. [b] Labels containing a letter following the primer length indicate a mismatched primer terminus. For example, 13T/20(C) indicates a 14/20mer with a 3'-terminal T·C mismatch.

Scheme I

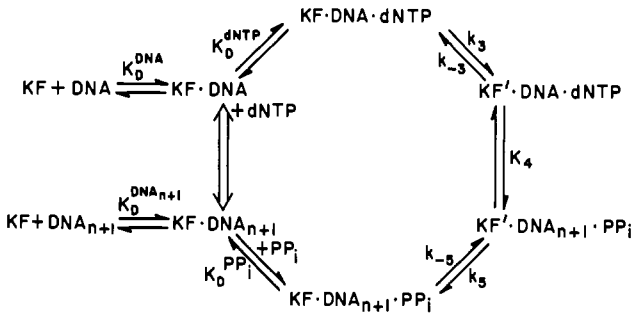

20 s on the rapid quench instrument.

Computer Simulations. Data were fit to exponential, hyperbolic, or linear functions by using the program RS1 (BBN Software Products Corp.). Simulations of kinetic mechanisms were performed with the program Simul (Barshop et al., 1983) as modified to accept data as *x,y* pairs (Anderson et al., 1988).

Results

The use of synthetic DNA duplexes made from oligonucleotides of defined sequences has allowed the definition of kinetic mechanisms for the incorporation of either correct or incorrect bases by KF. The synthetic duplexes used in this study are shown in Chart I. The kinetic scheme governing incorporation of incorrect bases previously defined in this laboratory (Kuchta et al., 1988) is shown in Scheme I. The current work extends this mechanism to define the pre-steady-state rates of misincorporation for all 12 possible mismatches by using a form of KF that is deficient in 3′–5′ exonuclease activity due to a double mutation in the exonuclease active site (Derbyshire et al., 1988). The use of the exo– mutant of KF is necessary because some of the misincorporation rates are slow enough so that the 3′–5′ exonuclease activity would otherwise mask them completely. The rates of incorporation of correct and incorrect bases by another mutant of KF, Y766S, that also is deficient in 3′–5′ exonuclease activity due to a second mutation, D424A, have also been determined.

Correct Incorporation. The kinetic mechanism for nonprocessive synthesis as determined previously is shown in Scheme II (Kuchta et al., 1987) and is used as the basis for comparison with Y766S. The kinetic parameters of correct

Scheme II

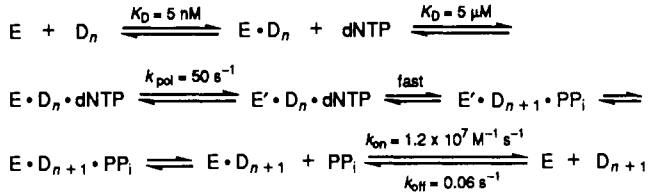

Table I: Kinetic Parameters for Correct Incorporation

	Y766S	KF
k_{cat} (s^{-1})	13[b]	50[a]
K_M(dATP) (μM)	7[b]	5[a]
k_{off}(DNA) (s^{-1})	0.11[b]	0.06[a]
K_D(DNA) (nM)	1.25[b]	5[a]
k_{exo}(9A/20) (s^{-1})	4.2×10^{-3}[c]	5×10^{-3}[d]

[a] From Kuchta et al. (1987). [b] Values were measured by using Y766S(exo–) and 13/20(T). [c] Value was measured by using Y766S(exo+) and 9A/20(A). [d] From Kuchta et al. (1988).

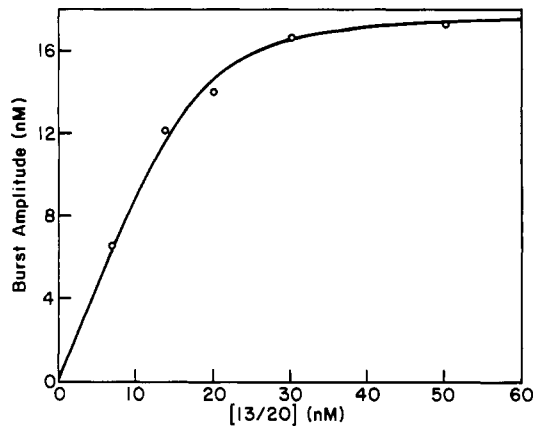

FIGURE 1: Binding of 13/20(T) to Y766S(exo–). The amount of bound enzyme·13/20(T) was measured as a function of the concentration of substrate DNA as described under Experimental Procedures. The calculated K_D was 1.25 nM.

incorporation are summarized in Table I. Like wild-type KF, Y766S displays a burst of synthesis on mixing enzyme·13/20(T) with Mg·dNTP equal to the amount of E·D complex present, followed by a slow rate that corresponds to the rate of release of product DNA. This facet of the mechanism is used to determine the thermodynamic binding constant for the E·D complex. Increasing amounts of 13/20(T) are added to a fixed concentration of Y766S, and the concentration of the E·D complex is determined by quantitating the burst amplitude. The plot of E·D versus 13/20(T) concentration is shown is Figure 1, and the data are fit to the quadratic form of the binding equation:

$$[E\cdot D] = \tfrac{1}{2}(E_0 + D_0 + K_D) - \sqrt{\tfrac{1}{4}(E_0 + D_0 + K_D)^2 - E_0D_0} \quad (1)$$

where E_0 represents the initial enzyme concentration, and D_0, the initial 13/20(T) concentration. The data were adequately fit by using a K_D of 1.25 nM. The result is somewhat lower than the reported value of 5 nM for wild-type KF and 13/20(T) (Kuchta et al., 1987), probably due to experimental uncertainties associated with working with such small quantities of substrate. Single-turnover reaction conditions were used to determine the rate of polymerization, k_{pol}, and K_M for dATP, shown in Table I. The efficiency of correct incorporation is somewhat reduced, 5-fold, for Y766S(exo–) relative to the wild type. The rate of 3′–5′ exonuclease activity was determined by using 9A/20(A) since the substrate existing

Table II: Misincorporation opposite Template G

sequence	incorporated base	enzyme	k_{cat}[a] (s^{-1})	K_M[a] (μM)	k_{cat}/K_M (M^{-1} s^{-1})	ratio,[b] mutant/wt
-GT	TTP	Y766S(exo-)	0.11	30	3700	44
-CAGGT-[c]		KF(exo-)	0.01	120	83	
-GT	TTP	Y766S(exo-)	0.21	49	4280	92
-CAGCT-[d]		KF(exo-)	6.7×10^{-3}	144	46	
-CT	dGTP	Y766S(exo-)	0.0054	10	540	4.1
-GAGCC-[d]		KF(exo-)	0.028	214	130	
-CT	dATP	Y766S(exo-)	0.023	33	690	2.7
-GAGCC-[d]		KF(exo-)	0.014	54	260	

[a] Calculated as described under Experimental Procedures. [b] Ratio of efficiencies, Y766S(exo-)/KF(exo-). [c] Sequence from the 10th position of the 9/20(A). [d] Sequence from the 14th position of the 13/20(G).

Table III: Misincorporation opposite Template T

sequence	incorporated base	enzyme	k_{cat}[a] (s^{-1})	K_M[a] (μM)	k_{cat}/K_M (M^{-1} s^{-1})	ratio,[b] mutant/wt
-GA	TTP	Y766S(exo-)	0.0075	175	43	3.3
-CTTCC-[c]		KF(exo-)	0.004	310	13	
-GA	dCTP	Y766S(exo-)	0.016	320	50	4.5
-CTTCC-[c]		KF(exo-)	0.013	1200	11	
-GA	dGTP	Y766S(exo-)	0.10	24	4200	8
-CTTCC-[c]		KF(exo-)	0.15	290	517	

[a] Calculated as described under Experimental Procedures. [b] Ratio of efficiencies, Y766S(exo-)/KF(exo-). [c] Sequence from 13/20(T).

after a misincorporation reaction would contain a 3′-terminal mismatch. The rate of 3′–5′ exonuclease activity is not significantly changed by the mutation, which is consistent with the distance between the 3′ exonuclease active site and Tyr766 (Ollis et al., 1984). Overall, the mutation only slightly alters the kinetics of correct incorporation.

Misincorporation. An important control was carried out to ensure that the appearance on the gel of a product band accurately reflects the incorporation of an incorrect nucleotide rather than the incorporation of a correct nucleotide that may have been present as a minor contaminant. The dNTP stocks used were of the highest purity commercially available. Gel electrophoresis can discriminate the small difference in mobility of oligonucleotides due to a difference only in the 3′-terminal base. In many cases, including the T·G mismatch, it was possible to separate mixtures of correctly extended primer oligonucleotides and those resulting from a misincorporation reaction. Because there is a physical difference between the two products, they cannot have the same sequence. Since, during the single-turnover reaction conditions employed, greater than 90% of the available substrate was turned into product (except for the slow misincorporations involving the misincorporation of a pyrimidine opposite a template pyrimidine), the observed rate cannot be due to a small amount of template having the complementary base to the added dNTP.

The substrates used in this work are shown in Chart I. A separate duplex was used for each set of misincorporation reactions, with a different base in the template position opposite the dNTP being incorporated. The surrounding sequences are similar among the duplexes used, though not identical, and so nearest neighbor effects are not identical for each misincorporation. Therefore, the trends in the kinetics of misincorporation must be considered valid only for the set of duplexes used in these experiments. However, comparisons between the mutant and the wild type for a given misincorporation are valid. The raw counts obtained from slicing product and substrate bands from the gel and counting them were normalized as a percentage of the total counts obtained for a given time point, thus eliminating differences due to loading slightly different volumes on the gel.

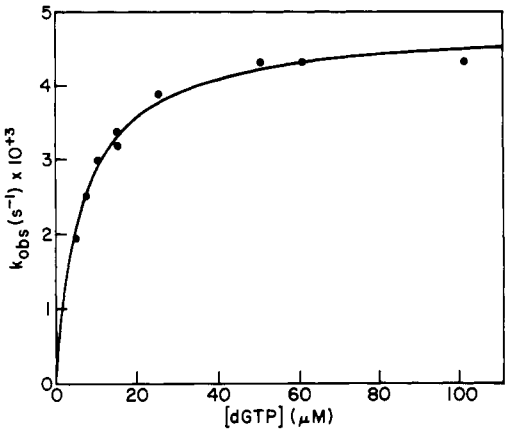

FIGURE 2: Rate of formation of a G·A mismatch by KF(exo-). Assays were performed under conditions of excess KF(exo-) over DNA substrate, 9/20(A), as described under Experimental Procedures.

Figure 2 demonstrates an important difference between KF and several other polymerases, for example, T7 (Wong et al., 1990) and pol α (Boosalis et al., 1987). The rate of misincorporation of dGTP opposite a template A can be saturated at relatively low concentrations of dGTP. This indicates that, during the polymerization event, KF discriminates against incorrect incorporation more by a reduction in the rate of incorporation than by an increase in the binding constant for the incorrect base. A direct proof of the saturation of all mismatches was not possible due to the high apparent K_M of some of the misincorporations and the inhibition of KF at high dNTP concentrations. However, in no case was the fidelity of replication due more to the increase in binding constant than the reduction in reaction rate. Direct measurement of the K_D for binding of mismatched nucleotides to KF·DNA binary complexes of various sequences also revealed little discrimination in the binding event (Eger et al., 1990).

Single-turnover reaction conditions in which there is an excess of enzyme over substrate DNA were employed to measure the rates of misincorporation. These conditions give rise to an exponential decrease in the amount of unreacted

Table IV: Misincorporation opposite Template A

sequence	incorporated base	enzyme	k_{cat}[a] (s^{-1})	K_M[a] (μM)	k_{cat}/K_M (M^{-1} s^{-1})	ratio,[b] mutant/wt
–CG –GCAGG–[c]	dCTP	Y766S(exo–) KF(exo–)	0.04 0.02	37 290	1080 68	16
–CG –GCAGG–[c]	dGTP	Y766S(exo–) KF(exo–)	0.0023 0.002	6 22	383 91	4.2
–CG –GCAGG–[c]	dATP	Y766S(exo–) KF(exo+)[d]	0.0034 0.035	37 40	92 880	0.1

[a] Calculated as described under Experimental Procedures. [b] Ratio of efficiencies, Y766S(exo–)/KF(exo–). [c] Sequence from 9/20(A). [d] From Kuchta et al. (1988).

Table V: Misincorporation opposite Template C

sequence	incorporated base	enzyme	k_{cat}[a] (s^{-1})	K_M[a] (μM)	k_{cat}/K_M (M^{-1} s^{-1})	ratio,[b] mutant/wt
–GT –CACAC–[c]	dCTP	Y766S(exo–) KF(exo–)	3.8×10^{-4} 7.9×10^{-5}	440 240	0.9 0.3	3
–GT –CACAC–[c]	dATP	Y766S(exo–) KF(exo–)	0.01 0.059	35 154	290 380	0.8
–GT –CACAC–[c]	TTP	Y766S(exo–) KF(exo–)	4.8×10^{-4} 1.5×10^{-3}	130 500	3.7 3	1.2

[a] Calculated as described under Experimental Procedures. [b] Ratio of efficiencies, Y766S(exo–)/KF(exo–). [c] Sequence from 13/20(C).

substrate with time, and the data were adequately fit by a single exponential. A double-reciprocal plot was then used to determine k_{cat} and K_M.

The wide range of rates and binding constants obtained for all misincorporation reactions is included in Tables II–V for both KF(exo–) and Y766S(exo–). For KF(exo–) the fastest misincorporation occurs for dGMP opposite template T at 0.15 s^{-1} and the slowest is for misincorporation of dCMP opposite template C at 7.9×10^{-5} s^{-1}, a range of 2×10^3. The value for correct incorporation is 50 s^{-1} (Kuchta et al., 1987). The lowest K_M for the KF(exo–) is 22 μM for reaction of dGTP opposite template A, and the highest K_M is estimated at 1.2 mM for misincorporation of dCTP opposite template T, a range of 50. The preference for misincorporation, as determined by order of decreasing efficiency (k_{cat}/K_M) for KF(exo–), with this set of duplexes is as follows: A·A, G·T, A·C, A·G, G·G, G·A, T·G, C·A, T·T, C·T, T·C, C·C (where the first base of each pair is being misincorporated opposite a template containing the second base of the pair), a range of 2.6×10^3. The general trend evident from these numbers is that KF more efficiently misincorporates purines opposite purines and wobble base pairs than it misincorporates pyrimidines opposite pyrimidines. The misincorporation efficiencies are asymmetrical. For instance, the efficiency of misincorporation of dCMP opposite a template A is 68 M^{-1} s^{-1} and that of dAMP opposite template C is 383 M^{-1} s^{-1}, a 5-fold difference.

The kinetics of misincorporation by Y766S(exo–) were also investigated by using the same experimental conditions, and several quantitative differences were noted. The overall range of rates of misincorporation remained similar to the range for KF(exo–). The most rapid misincorporation was for TMP opposite template G occuring at 0.11 s^{-1}, and the slowest rate of misincorporation, as for KF(exo–), was for misincorporation of dCMP opposite a template C at 3.8×10^{-4} s^{-1}. The range of values for K_M for Y766S(exo–) was slightly decreased compared to that for KF(exo–), from 6 μM for misincorporation of dGMP opposite a template A to 440 μM for misincorporation of dCMP opposite template C. It is interesting to note that the K_M values of misincorporation of a given dNMP opposite any template base fall into very narrow ranges for Y766S(exo–) following the trend $K_M(G) < (A) < (T) < (C)$, with average values for K_M of $13 < 34 < 110 < 265$ μM, respectively. For KF(exo–) the order of increasing average K_M is $A < G < T < C$, $82 < 175 < 309 < 576$ μM, respectively. However, there is much greater variance in the K_M values for each base for KF(exo–). The range of efficiency of misincorporation for Y766S(exo–) has a high value of 4200 M^{-1} s^{-1} for T·G and a low of 0.33 M^{-1} s^{-1} for misincorporation of C·C.

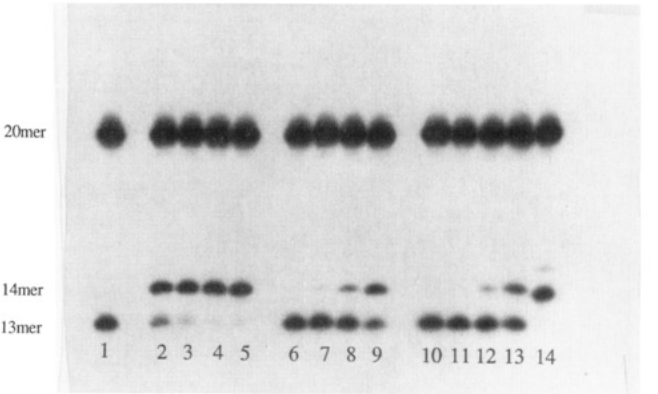

FIGURE 3: Misincorporation of TMP opposite template G. All assays included 30 μM TTP, 115 nM 13/20(G), 50 mM Tris, pH 7.4, and 5 mM $MgCl_2$. The mismatch was catalyzed by 400 nM Y766S(exo–) (lanes 2–5), Y766F(exo–) (lanes 6–9), or KF(exo–) (lanes 10–13). After reaction times of 15 s (lanes 2, 6, and 10), 1 min (lanes 3, 7, and 11), 5 min (lanes 4, 8, and 12), or 20 min (lanes 5, 9, and 13), aliquots were withdrawn, quenched in gel load buffer, and subjected to gel electrophoresis and autoradiography. Lane 1 is the 13/20(G) alone. Lane 14 is the product of correct synthesis [13/20(G) + dCTP].

The ratio of misincorporation efficiency of Y766S(exo–) to that of KF(exo–) is a measure of the change of fidelity for a given mismatch on creation of the mutation. The largest ratios are for T·G (44), C·A (16), and G·T (8). The misincorporation of T opposite template G was also measured in a slightly different sequence context, the 14th position of 13/20(G), and the ratio was found to be 92 (Table II). Figure 3 illustrates the difference in the misincorporation rates for Y766S(exo–), Y766F(exo–), and KF(exo–). After 15 s of reaction, almost all of the substrate has been turned over by Y766S(exo–) but little or no product is visible for the reactions catalyzed by Y766F(exo–) or KF(exo–). All but two of the other misincorporations showed only very modest increases in

Table VI: Steady-State Misincorporation

template	incorporated base	enzyme	k_{cat}[a] (s^{-1})	K_M[a] (μM)	k_{cat}/K_M (M^{-1} s^{-1})	ratio
-GT	TTP	Y766S(exo-)	8×10^{-3}	11	720	51[c]
-CAGGT-[b]		KF(exo-)	7.2×10^{-4}	50	14	
		Y766F(exo-)[d]	8.7×10^{-4}	96	9.1	0.65[e]

[a] Calculated as described under Experimental Procedures. [b] Sequence from 9/20(A). [c] Ratio of efficiencies, Y766S(exo-)/KF(exo-). [d] Measured by using 13/20(G). [e] Ratio of efficiencies, Y766F(exo-)/KF(exo-).

efficiency. The only mismatches displaying decreased efficiency of misincorporation caused by the mutation are A·C (0.8) and A·A (0.1). The effect of the mutation on the misincorporation efficiencies was not symmetrical. For example, the increase for T·G was 44-fold while that of G·T was only 8-fold. For purposes of comparison of the kinetic parameters of catalysis between mutant and wild-type polymerases, a ratio of 4 or greater is probably kinetically significant, due to uncertainties in the measurement of the reaction rates.

The steady-state rate of misincorporation is determined by the rate of a conformational change occurring after the chemical step (Kuchta et al., 1988). The conformational change is designated k_5 in Scheme I. To determine if the same differences between Y766S(exo-) and KF(exo-) that were observed in the pre-steady-state also hold true under the steady-state conditions, k_5 was measured for the misincorporation of TMP opposite template G, the misincorporation with the largest change in efficiency due to the mutation. The results are shown in Table VI. Y766S(exo-) exhibits an increase in the steady-state rate of misincorporation and a decrease in the K_M for TTP that closely mimic the changes between the pre-steady-state kinetic constants for Y766S(exo-) and KF(exo-). The fact that the pre-steady-state rate of misincorporation is greater than the steady-state rate demonstrates that this facet of the overall mechanism of misincorporation holds for Y766S(exo-) despite quantitative differences in the rate constants. The K_M for the pre-steady-state rate is substantially greater than the K_M for the steady-state rate because the pre-steady-state K_M reflects the true dissociation constant for the dNTP since it was derived from single-turnover conditions and the steady-state K_M reflects the saturation of the k_5 rate only.

To show that the effects of the changes in the rates of misincorporation as measured with the exo- forms of Y766S and KF are seen with Y766S(exo+) and wild-type KF, the rate and extent of buildup of the T·G mismatch in the presence of excess Y766S and KF were determined. Figure 4 displays the results. The extent of buildup of the mismatched product is 10-fold greater in the presence of Y766S compared to KF, despite the concentration of TTP being 7% of K_M for Y766S and 33% of K_M for KF. Higher concentrations of TTP with Y766S result in complete conversion of all available substrate into mismatched product (data not shown). The difference in the amount of mismatched product at steady state is a consequence of the higher ratio of k_5/k_{exo} for Y766S relative to KF, and not to a reduced k_{exo} (Table I).

Another consequence of the changes in the k_5 rate is the difference observed in the steady-state rate of dNTP turnover, which occurs by a mechanism of incorporation and then excision by the 3′–5′ exonuclease activity (Mizrahi et al., 1986). The results for two different misincorporation reactions are shown in Table VII. The observed rate of production of dNMP may be limited by either the rate of misincorporation or the rate of 3′–5′ exonuclease activity. With Y766S and the misincorporation of TMP opposite template G, the rate of misincorporation in the steady state is rapid relative to the exonuclease rate so the observed rate is limited by the maximum exonuclease activity. The opposite is the case with KF and T·G, so the observed rate is close to the misincorporation rate. With the misincorporation of dATP opposite template A as catalyzed by Y766S, the observed rate is limited by the steady-state misincorporation rate and is less than the full 3′ exonuclease activity. KF makes the same misincorporation more rapidly, and so the full exonuclease activity is observed.

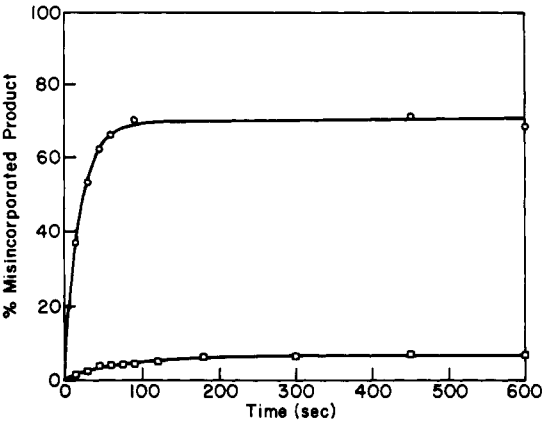

FIGURE 4: Buildup of misincorporated product in the presence of excess exo+ enzymes. Reaction conditions were as described under Experimental Procedures for Y766S(exo+) (○) and for KF (□), catalyzing the misincorporation of TMP into 13/20(G) with TTP at 2.5 μM for Y766S(exo+) and at 40 μM for KF.

Table VII: dNTP Turnover at 10 μM dNTP[a]

template	dNTP	Y766S(exo+) k_{obs} (s^{-1})	KF k_{obs} (s^{-1})
13/20(G)	TTP[b]	4.2×10^{-3}	4.2×10^{-4}
9/20	dATP[c]	4.5×10^{-4}	1.9×10^{-3}

[a] Rates were calculated as pmol of dNMP produced s^{-1} (pmol of enzyme)$^{-1}$. [b] Forms a T·G mismatch. [c] Forms an A·A mismatch.

In order to incorporate a mismatch stably, the polymerase must be able to add correct bases onto the mismatch. The ability of Y766S to carry out this extension was investigated by using two different mismatches: 13T/20(C), in which the next correct base is also a T, and 13G/20(T), in which the next correct base is a G. The extensions of these mismatches were carried out under conditions of excess exo- enzyme, and the results are shown in Figure 5 for extension of the T·C mismatch. KF extends the T·C mismatch more rapidly than it makes the mismatch, and therefore the band corresponding to the mismatched product is very faint on the gel (Figure 5A). In contrast, Y766S makes the T·C mismatch more rapidly than it can extend the mismatch, so a prominent band corresponding to the mismatched intermediate appears on the gel. The rates of appearance and disappearance of the intermediate T·C mismatch and the extended product are adequately fit by Scheme III. The rate of the formation of the mismatch was determined as the rate of the disappearance of the substrate. The rate of extension of T·C was determined by using a preformed mismatch made with synthetic oligonucleotides, and the rates are shown in Table VIII. The difference in product distribution between KF(exo-) and Y766S(exo-) is due to the

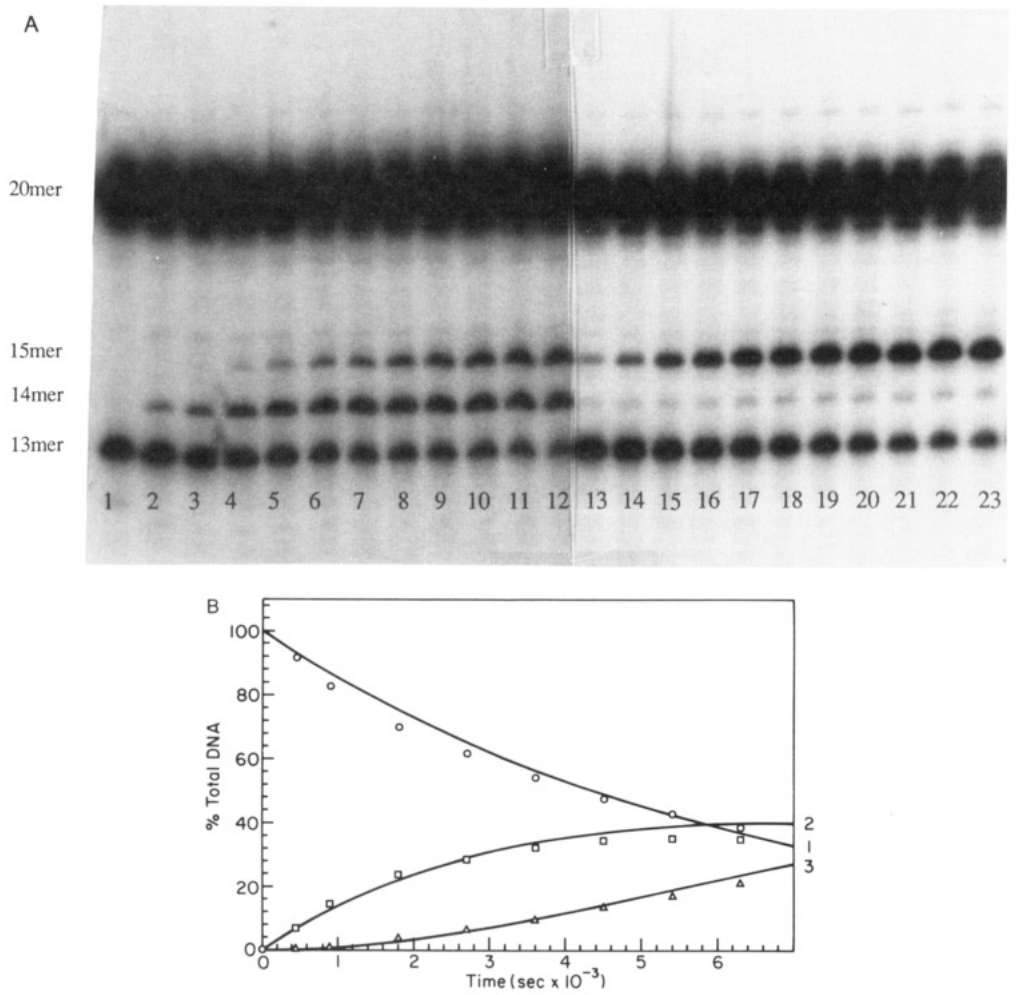

FIGURE 5: (A) Simultaneous misincorporation and extension of a T·C mismatch. Reaction conditions included 100 μM TTP, 105 nM 13/20(C), 50 mM Tris, pH 7.4, 5 mM $MgCl_2$, and 400 nM Y766S(exo−) (lanes 2–12) or KF(exo−) (lanes 14–24). After reaction times of 7.5, 15, 30, 45, 60, 75, 90, 105, 120, 135, and 150 min (lanes 2–12, respectively) or 0.25, 0.5, 1, 2, 3, 4, 5, 7.5, 10, 20, and 30 min (lanes 13–23, respectively), aliquots were quenched in gel loading buffer, electrophoresed, and subjected to autoradiography. (B) Simulation of the formation and extension of the T·C mismatch by Y766S(exo−). Conditions were as described for panel A. The rate of disappearance of 13/20(C) (○), appearance of 14/20(C) (□), and the extended 15/20(C) (△) were simulated by using Kinsim as described under Results. The rate of misincorporation was 2×10^{-4} and of extension was 1.2×10^{-4} s^{-1}.

Table VIII: Formation and Extension of a Mismatch

$$13/20(C) + TTP \xrightarrow{k_1} 13T/20(C) + TTP \xrightarrow{k_2} 13TT/20(C)$$

	k_1[a]				k_2[b]			
	k_{cat} (s^{-1})	K_M (μM)	k_{cat}/K_M (M^{-1} s^{-1})	ratio[c]	k_{cat} (s^{-1})	K_M (μM)	k_{cat}/K_M (M^{-1} s^{-1})	ratio[c]
Y766S(exo−)	4.8×10^{-4}	130	3.7	1.2	1.6×10^{-4}	12	13	0.008
KF(exo−)	1.5×10^{-3}	500	3		2.7×10^{-2}	16	1700	

[a] Rates were determined by using 13/20(C). [b] Rates were determined by using 13T/20(C). [c] Ratio of efficiencies, Y766S(exo−)/KF(exo−).

differences in the rate of formation and the rate of extension of the mismatch. The elemental effect on the extension of the T·C mismatch was determined to be in the range of 7–10 for both KF(exo−) and Y766S(exo−), indicating the possible inclusion of some part of the chemical step in the observed rate.

Scheme III

$$E{\cdot}13/20(C) \rightarrow E{\cdot}13T/20(C) \rightarrow E{\cdot}13TT/20(C)$$

The extension of G·T was also examined by using 13G/20(T). Biphasic reaction progress curves were observed with both KF(exo−) and Y766S(exo−) under single-turnover conditions (data not shown). The rate of extension of G·T by Y766S(exo−) was 4-fold slower than the rate of extension of G·T by KF(exo−) in the slow phase (0.06 s^{-1} vs 0.24 s^{-1}). Therefore, the quantitative effect of the Y766S mutation on the extension of mismatches varies greatly depending on the mismatch. Experiments to determine the nature of the biphasic extension of G·T are in progress.

The kinetic parameters of misincorporation for several mismatches as catalyzed by Y766F(exo−) are summarized in Table IX. Overall, there is very little difference in the efficiencies of misincorporation between KF(exo−) and Y766F(exo−) for the mismatches examined, which include the T·G mismatch which showed the greatest increase in efficiency of formation on creation of the Y766S mutation. The steady-state rate of misincorporation by Y766F(exo−) for the T·G mismatch is also similar to that for KF(exo−) (Table VI).

Discussion

These studies were initiated as part of a continuing effort to understand the mechanism by which KF so accurately carries out synthesis of DNA. Prior work has led to the

Table IX: Kinetic Parameters of Misincorporation by Y766F(exo–)

sequence	base	k_{cat} (s^{-1})[a]	K_M (μM)[a]	k_{cat}/K_M (M^{-1} s^{-1})	ratio[b]
–T –AGCC–[c]	TTP	3.9×10^{-3}	81	48	1.0
–T –AGCC–[c]	dATP	5.4×10^{-3}	72	75	0.31
–A –TTCC–[d]	dGTP	2.3×10^{-2}	64	360	0.70
–A –TTCC–[d]	TTP	2.6×10^{-3}	220	12	0.93
–A –ACAC–[e]	dATP	1.2×10^{-2}	99	121	0.32
–A –TTCC–[d]	dATP	70	6.7	1.0×10^{7}	1.0

[a] Measured as described under Experimental Procedures. [b] Ratio of efficiencies, Y766F(exo–)/KF(exo–). [c] Sequence from 13/20(G). [d] Sequence from 13/20(T). [e] Sequence from 13/20(C).

development of a kinetic mechanism describing three distinct kinetic steps that serve to increase the discrimination against incorrect nucleotides. They include discrimination during nucleotide binding and phosphodiester bond formation; a kinetic pausing step, k_5 in Scheme I, that serves to hold mismatches onto the enzyme allowing additional time for the 3′–5′ exonuclease activity to function; and classical proofreading, which is removal of 3′-terminal mismatches by the 3′–5′ exonuclease, which is increased due to the slow addition of the next correct nucleotide onto a mismatch. Overall, if the enzyme functions optimally, the selectivity is in the range of 2×10^{10} bases replicated per error. Of this, approximately 10^6 could be ascribed to selectivity during stage I, the polymerization event. The use of single-turnover conditions and a form of KF that is devoid of the 3′ exonuclease activity due to mutations in the 3′–5′ exonuclease active site (Derbyshire et al., 1988) limits the observed selectivity in this work to that which occurs only during the polymerization event. In order to understand variations in selectivity for all misincorporations and to gain insight into the possible roles of individual amino acids of the enzyme, the study of site-specific mutants of KF was undertaken. One mutant, Tyr766Ser, displayed significant changes in the kinetics of misincorporation for several mismatches.

To serve as a basis for comparison with site-specific mutants, the kinetic mechanism of misincorporation was extended to cover all 12 possible mismatches formed by KF. KF(exo–) can catalyze the formation of all 12 mismatches at observable rates. The rates of misincorporation vary from 0.1 s^{-1} for G·T to 10^{-4} s^{-1} for C·C. The general trend in the order of the efficiencies of misincorporation by KF(exo–) indicates the most easily formed mismatches are wobble base pairs and purines opposite purines and the most difficult mismatches to form are those with pyrimidine opposite pyrimidine. Therefore, transversion mutations formed by KF that result from replacement of pyrimidine·purine with purine·pyrimidine are much more likely to occur through an intermediate involving a purine·purine mismatch than through a pyrimidine·pyrimidine mismatch. Several misincorporation reactions had K_M values greatly increased relative to correct incorporation. For example, for C·C the K_M was estimated at 1.2 mM, an increase of 240-fold over the K_M for correct incorporation of 5 μM. Because of the high values for K_M it was not possible to demonstrate conclusively the saturation of the misincorporation rate due to the inhibition of the polymerase at high dNTP concentrations. The cases of increased K_M all occurred with the misincorporation of pyrimidine·pyrimidine, indicating the decreased binding of incorrect pyrimidines plays a greater part in increasing fidelity than does the decrease in binding of purines.

Even in cases of greatly increased K_M for misincorporation, the decrease in the rate of reaction predominates in selectivity. For example, for T·C, the K_M increased 100-fold while the rate of incorporation decreased 34 000-fold, while for C·T, the K_M increased 240-fold while the rate decreased 3800-fold. In contrast, the selectivity of pol α has been attributed largely to an increase in the K_M for incorrect dNTP (Boosalis et al., 1987). However, the differences in K_M vs V_{max} discrimination and the results from the single-turnover experiments presented here cannot be directly compared due to the complexity of the expressions contained in the kinetic parameters of K_M and V_{max} as determined by steady-state methods (Boosalis et al., 1987). The polymerases of phages T4 and T7 have both been shown to have greatly increased binding constants for incorrect dNTP's. In the case of T4 polymerase, the increased K_M for incorrect dNTP was inferred from the absence of a decrease in the rate of correct incorporation in the presence of a high concentration of incorrect nucleotide (T. Capson, personal communication). A mutant of T7 polymerase with no 3′ exonuclease activity shows no evidence of saturation of the misincorporation rate even at millimolar concentrations of incorrect dNTP (Wong et al., 1990). Thus, of the polymerases that have been examined by pre-steady-state methods to date, only KF shows selectivity by a decrease in the rate of misincorporation instead of an increase in the binding of incorrect dNTP. Variations in the quantitative amount of increase in the binding constant for an incorrect dNTP have been noted for pol I and KF (Fersht, 1983; El-Deiry, 1984). These differences may be due to template and nearest-neighbor effects (Mendelman et al., 1989) and may be due, in part, to kinetic differences of each mismatch reaction mechanism.

Significant quantitative changes in the kinetic parameters governing several misincorporations are created with the conversion of Tyr766 to Ser. Depending on the mismatch, K_M, k_{cat}, or both parameters show significant increases or decreases. Therefore, Tyr766 probably does not interact with each incoming incorrect dNTP in the same manner. In general though, the K_M's for misincorporation by Tyr766Ser are lower than those for KF. The mutant has an altered order of decreasing efficiencies of misincorporation, and the three mismatches that show the largest increase in efficiency of formation are T·G, C·A, and G·T, all purine opposite pyrimidine. The misincorporations of dATP opposite any template base are the only mismatches for which the efficiency is decreased for Y766S, though overall, since the efficiency of correct incorporation is also decreased, the fidelity of incorporation is largely unchanged.

The observed increase in the rate of misincorporation of TMP opposite template G with Y766S under single-turnover conditions in the absence of 3′ exonuclease activity constitutes proof of the active participation of KF(exo–) in reducing this misincorporation during the polymerization event. Therefore, the high fidelity observed with KF is not solely a result of mismatch structural instability relative to correctly base-paired duplex DNA or solely to kinetic events subsequent to polymerization such as mismatch editing. Specifically for the mismatch T·G, stage I selectivity, as previously defined (Kuchta et al., 1988), is 10^7 M^{-1} s^{-1} (correct)/83.3 M^{-1} s^{-1} (incorrect) = 1.2×10^5 for KF. Y766S has for the same mismatch a selectivity of 1.8×10^6 M^{-1} s^{-1} (correct)/3333 M^{-1} s^{-1} (incorrect) = 540. The decrease in selectivity is therefore 220-fold for the T·G mismatch. By contrast, for the A·A mismatch, KF has a fidelity ratio of 10^4 and Y766S has a ratio

of 2×10^4, a 2-fold increase in fidelity for Y766S.

To determine if the increased efficiencies of misincorporation for Y766S(exo−) were due to the loss of the phenolic ring of the Tyr766 side chain or to the loss of its phenolic hydroxyl, several misincorporations as catalyzed by Y766F(exo−) were examined, including T·G which showed the largest increase in efficiency of misincorporation for Y766S(exo−). The efficiencies of misincorporation catalyzed by Y766F(exo−) were not greatly different from those of KF(exo−), indicating that it is the loss of the phenolic ring of Tyr766 that causes the observed decrease in fidelity of DNA synthesis.

Subsequent kinetic events in the mechanism of misincorporation are also affected by the mutation Y766S. The efficiency of the second conformational change, designated k_5 in Scheme I, was increased 51-fold for Y766S(exo−) for the T·G mismatch, allowing a more rapid steady-state rate of misincorporation. The rate of extension of a mismatch is also affected by the mutation. The rate of extension of a T·C mismatch was decreased 170-fold for Y766S(exo−) while the rate of extension of a G·T mismatch was decreased 4–6-fold.

The structure of duplex DNA containing mismatched base pairs has been investigated by X-ray crystallographic (Brown et al., 1985; Kennard, 1985) and two-dimensional NMR techniques [e.g., Patel et al. (1987)]. No global changes in the structure were noted, but alterations in the area immediately adjacent to the mismatched bases were observed. For a B-form duplex containing a T·G wobble mismatch, the base overlap on the 5′ side of the T was greater than normal overlap in B-DNA and the overlap on the 3′ side of the T was less than normal overlap. The base overlap on the G-containing strand was not significantly different. The increased overlap 5′ of the T may explain, in part, the asymmetry observed in the efficiencies of misincorporation of a given mismatch. For example, misincorporation of T opposite template G is 5-fold more efficient than misincorporation of G opposite template T. The decreased overlap 3′ to the T may be part of the cause of the decreased rate of extension of the mismatch relative to the rate of extension of correct base pairs.

The physical–chemical role of the Tyr766 side chain in reducing misincorporation efficiencies remains obscure. One possibility is a direct interaction between the phenolic side chain and the incoming incorrect dNTP. The interaction could be either steric through involvement of the phenolic side chain or by hydrogen-bonding interaction with the phenolic hydroxyl. Since the misincorporation efficiency of Y766F(exo−) for the T·G mismatch is similar to that of KF(exo−), it is the loss of the phenolic side chain that causes the increase in misincorporation of T·G. Exclusion of water from the active site by the side chain of Tyr766 would serve to increase the energy difference between correctly and incorrectly base-paired duplexes (Petruska et al., 1986). The differential effects of the mutation on different mismatches may be a result of differential abilities of the α-phosphate of the incoming incorrect dNTP, in the absence of the Tyr766 side chain, to approach the position of the α-phosphorus during correct incorporation. Discerning which of these alternatives is correct must await more detailed structural information.

The kinetic parameters derived by pre-steady-state methods in this work are consistent with the mutator phenotype of cells harboring a Y766S, D424A allele (Polesky et al., 1990). Thus, these experiments can serve as a bridge between the two methods of detecting changes in fidelity. The strict conservation of Tyr766 among polymerases from *Streptococcus pneumonia*, *Thermus aquaticus*, *E. coli*, and phage T5 (Lawyer et al., 1989; Leavitt & Ito, 1989; Lopez et al., 1989) argues for a similar role for this residue in those polymerases. The possibility of other residues serving a similar function for other mismatches is currently being investigated by using site-directed mutagenesis.

Registry No. Pol I, 9012-90-2; L-Tyr, 60-18-4; dATP, 1927-31-7; 9/20(A), 111378-64-4; 13/20(T), 111378-65-5; 13/20(G), 130727-08-1; 13/20(C), 130727-05-8; 9A/20(A), 115912-00-0; 13T/20(C), 130727-06-9; 13G/20(T), 130727-07-0; dGTP, 2564-35-4; dCTP, 2056-98-6; TTP, 365-08-2.

References

Anderson, K. S., Sikorski, J. A., & Johnson, K. A. (1988) *Biochemistry 27*, 7395–7406.

Barshop, B. A., Wrenn, R. F., & Frieden, C. (1983) *Anal. Biochem. 130*, 134–145.

Boosalis, M. S., Petruska, J., & Goodman, M. F. (1987) *J. Biol. Chem. 262*, 14689–14696.

Brown, T., Kennard, O., Kneale, G., & Rabinovich, D. (1985) *Nature 315*, 604–606.

Brutlag, D., Atkinson, M. R., Setlow, P., & Kornberg, A. (1969) *Biochem. Biophys. Res. Commun. 37*, 982–989.

Bryant, F. R., Johnson, K. A., & Benkovic, S. J. (1983) *Biochemistry 22*, 3537–3546.

Catalano, C. E., Allen, D. J., & Benkovic, S. J. (1990) *Biochemistry 29*, 3612–3621.

Derbyshire, V., Freemont, P. S., Sanderson, M. R., Beese, L. S., Friedman, J. M., Steitz, T. A., & Joyce, C. M. (1988) *Science 240*, 199–201.

El-Deiry, W., Downey, K. M., & So, A. G. (1984) *Proc. Natl. Acad. Sci. U.S.A. 81*, 7378–7382.

Fersht, A. R., Shi, J.-P., & Tsui, W.-C. (1983) *J. Mol. Biol. 165*, 655–667.

Johnson, K. A., (1986) *Methods Enzymol. 134*, 677–705.

Joyce, C. M., & Grindley, N. D. F. (1983) *Proc. Natl. Acad. Sci. U.S.A. 80*, 1830–1834.

Joyce, C. M., Ollis, D. L., Rush, J., Steitz, T. A., Konigsberg, W. H., & Grindley, N. D. F. (1985) In *Protein Structure, Folding and Design* (Oxender, D., Ed.) UCLA Symposia on Molecular and Cellular Biology 32, pp 197–205, Alan R. Liss, New York.

Kennard, O. (1985) *J. Biomol. Struct. Dyn. 3*, 205–226.

Klenow, H., & Henningsen, I. (1970) *Proc. Natl. Acad. Sci. U.S.A. 65*, 168–175.

Kuchta, R. D., Mizrahi, V., Benkovic, P. A., Johnson, K. A., & Benkovic, S. J. (1987) *Biochemistry 26*, 8410–8417.

Kuchta, R. D., Benkovic, P., & Benkovic, S. J. (1988) *Biochemistry 27*, 6716–6725.

Lawyer, F. C., Stoffel, S., Randall, K. S., Myambo, K., Drummond, R., & Gelfond, D. H. (1989) *J. Biol. Chem. 264*, 6427–6437.

Leavitt, M. C., & Ito, J. (1989) *Proc. Natl. Acad. Sci. U.S.A. 86*, 4465–4469.

Lopez, P., Martinez, S., Diaz, A., Espinose, M., & Lacks, S. A. (1989) *J. Biol. Chem. 264*, 4255–4263.

Maniatis, T., Fritsch, E. I., & Sambrook, J. (1982) *Molecular Cloning. A Laboratory Manual*, Cold Spring Harbor Laboratory, Cold Spring Harbor, NY.

Mendelman, L. V., Petruska, J., & Goodman, M. F. (1990) *J. Biol. Chem. 265*, 2338–2346.

Mizrahi, V., Benkovic, P., & Benkovic, S. J. (1986) *Proc. Natl. Acad. Sci. U.S.A. 83*, 5769–5773.

Ollis, D. L., Brick, P., Hamlin, R., Xuong, N. G., & Steitz, T. A. (1985) *Nature 313*, 762–766.

Patel, D. J., Shapiro, L., & Hare, D. (1987) *Nucleic Acids and Molecular Biology* (Eckstein, F., & Lilley, D. M. J., Eds.) Vol. 1, pp 70–84, Springer-Verlag, New York.

Perrino, F. W., & Loeb, L. A. (1989) *J. Biol. Chem. 264*, 2898-2905.
Petruska, J., Sowers, L. C., & Goodman, M. F. (1986) *Proc. Natl. Acad. Sci. U.S.A. 83*, 1559-1562.
Polesky, A., Steitz, T. A., Grindley, N. D. F., & Joyce, C. M. (1990) *J. Biol. Chem.* (submitted for publication).
Setlow, P., Brutlag, D., & Kornberg, A. (1972) *J. Biol. Chem. 247*, 224-231.
Wong, I., Patel, S., Donlin, M., & Johnson, K. (1990) *Biochemistry* (submitted for publication).

Upstream Sequence Activation of *Escherichia coli argT* Promoter in Vivo and in Vitro†

Lilian M. Hsu,*,‡ Jacqueline K. Giannini,‡ Tsui-Wah C. Leung,‡ and James C. Crosthwaite§
Program in Biochemistry, Mount Holyoke College, South Hadley, Massachusetts 01075, and Department of Chemistry, University of North Carolina at Charlotte, Charlotte, North Carolina 28223
Received February 27, 1990; Revised Manuscript Received August 30, 1990

ABSTRACT: *Escherichia coli argT* promoter in a *galK* fusion construct is shown by BAL 31 deletion to require its upstream region for high in vivo activity. The extent of activation conferred by the upstream sequence from −130 to −38 is 25-fold. A spontaneous mutant containing a T to G transversion at −37 (i.e., the T-37G promoter) shows a similar requirement; however, the upstream sequence producing a 10-fold effect spans only −130 to −60. The difference in upstream sequence boundaries between the wild-type and T-37G promoters suggests the possible existence of two activating elements. Gel mobility investigation points to the presence of bent DNA in the *argT* promoter, and the bent center was localized to the −90 to −95 region by circular permutation analysis. The role of the upstream activating sequence (UAS) in promoter function was probed by competitive transcription experiments in vitro. Results of this type of analysis indicate that the full UAS activates transcription through a combined effect on K_B and k_2. Of these, K_B is significantly strengthened by the proximal element, and k_2 is stimulated to a smaller extent by the distal element. The evidence from deletion analysis, gel mobility investigation, and competitive transcription together support a "two-element" model of UAS function for the *argT* promoter.

To probe the regulation of a gene, it is necessary to first understand the activity of its promoter. Research over the past decade has made clear that many of the signals of regulation reside within the promoter region. Prokaryotic promoters recognized by $E\sigma^{70}$ have been shown to contain two hexameric consensus elements at the −35 and −10 regions separated optimally by 17 base pairs (bp)[1] of spacer DNA (Rosenberg & Court, 1979; Siebenlist et al., 1980; Hawley & McClure, 1983; Harley & Reynolds, 1987). Abundant biochemical and genetic analyses point to these elements as the recognition signals for RNA polymerase binding to the promoter [reviewed by McClure (1985)]. RNA polymerase σ-subunit mutations that compensate for changes in the consensus nucleotides further substantiate the role of these hexameric sequences in transcription initiation (Helmann & Chamberlin, 1988; Gardella et al., 1989; Siegele et al., 1989; Zuber et al., 1989).

For many phage and cellular messenger RNA promoters, a direct correlation has been demonstrated in vitro between the facility of open complex formation, as measured by the product K_Bk_2, and the agreement of the hexameric sequences to consensus, as meausred by the homology score (Mulligan et al., 1984). This relationship suggests that the consensus nucleotides provide the maximum fit in promoter–polymerase binding. On the basis of the K_Bk_2 values, this diverse set of promoters can be ordered on a scale of intrinsic selectivity by RNA polymerase that varies over 4 orders of magnitude (Mulligan et al., 1984).

A subset of the above promoters has also been analyzed systematically in vivo (Bujard et al., 1987). The comparison reveals a lack of correspondence between the in vivo promoter strength and the promoter hierarchy established in vitro (Deuschle et al., 1986). For example, *tac*, the synthetic consensus promoter, was found not to be the most active promoter in vivo (Bauer et al., 1988; Bujard et al., 1987); instead, it was shown that sequences downstream from +1 can play a significant role in determining activity. This finding coupled with the realization that no naturally occurring *E. coli* promoters utilize the consensus sequence led to the suggestion that promoter activities are optimized, rather than maximized, in vivo (McClure, 1985; Bujard et al., 1987).

Many factors have been found to contribute to promoter optimization in vivo, some exerting generalized effects while others influencing unique sites. These factors include the role of activator and repressor proteins, the degree of template

† This work was supported by grants from the Research Corp. (C1466) and National Institutes of Health (GM-40181) and by faculty grants from Mount Holyoke College. Partial support for this work has also been provided by the National Science Foundation's College Science Instrumentation Program (Grant CSI-8650956).
‡ Mount Holyoke College.
§ University of North Carolina at Charlotte.

[1] Abbreviations: OAc, acetate; amp, ampicillin; ATP, adenosine 5′-triphosphate; bp, base pair(s); BSA, bovine serum albumin; CMP, cytidine 5′-monophosphate; CTP, cytidine 5′-triphosphate; DTT, dithiothreitol; EtdBr, ethidium bromide; Na_2EDTA, ethylenediaminetetraacetic acid disodium salt; gal, galactose; GalK, galactokinase; gal-1-P, galactose 1-phosphate; GTP, guanosine 5′-triphosphate; HEPES, 4-(2-hydroxyethyl)-1-piperazineethanesulfonic acid; KGlu, potassium glutamate; nt, nucleotide(s); NTP, ribonucleoside triphosphate; PAGE, polyacrylamide gel electrophoresis; PolIk, DNA polymerase I Klenow fragment; RNAP, RNA polymerase; rms, root mean square; SD, standard deviation; Tris, tris(hyroxymethyl)aminomethane; UAS, upstream activating sequence; UTP, uridine 5′-triphosphate; XC, xylene cyanol.

0006-2960/91/0430-813$02.50/0